American Mineralogist, Volume 82, pages 345–353, 1997

A new garnet-orthopyroxene thermometer based on reversed Al_2O_3 solubility in FeO-Al_2O_3-SiO_2 orthopyroxene

L.Y. Aranovich[1,*] and R.G. Berman[2]

[1]Department of the Geophysical Sciences, University of Chicago, Chicago, Illinois, 60637, U.S.A.
[2]Geological Survey of Canada, 601 Booth Street, Ottawa, Ontario, Canada K1A 0E8

Abstract

Reversed phase-equilibrium data, collected over the *P-T* range 12–20 kbar at 850–1100 °C, define the solubility of Al_2O_3 in ferrosilite (Fs) in equilibrium with almandine garnet (Alm). The new data indicate significantly lower Al_2O_3 solubility in Opx in the Fe-bearing system compared with the Mg-system and extrapolate well to merge with the higher pressure bracket of Kawasaki and Matsui (1983). Orthopyroxene-garnet thermometry in crustal rocks, based on the equilibrium studied here (Alm = 3 Fs + Al_2O_3), is considerably more robust than previous calibrations based on the equivalent equilibrium in the Mg system. Results for several granulite terrains show that Al-Opx temperatures based on the new experimental data are generally higher than results based on Fe-Mg exchange thermometry, consistent with suggestions of previous workers. For many samples, the difference in apparent closure temperature between these equilibria (generally 50–130 °C) is within the combined uncertainty of their calibration (~75 °C) and is not as extreme as differences calculated on the basis of Harley's (1984) unreversed experimental data (Bégin and Pattison 1994). The lack of sensitivity of this new thermometer to late Fe-Mg exchange makes it a powerful tool for deciphering near-peak *P-T* conditions for high-grade rocks.

Introduction

The Al_2O_3 content in orthopyroxene coexisting with garnet in various rock types is recognized as a sensitive indicator of the pressure (*P*)-temperature (*T*) conditions at which rocks equilibrated. Initial experimental investigations focused on the simplest chemical system, MgO-Al_2O_3-SiO_2 (MAS), in order that *P-T* estimates could be derived for ultramafic, upper-mantle xenoliths (e.g., Boyd 1973). More recent interest in Opx-Gt thermobarometry stems from attempts to understand lower crustal processes by defining metamorphic conditions for granulite facies rocks. Of fundamental importance to these endeavors are inferences that the Al_2O_3 content of Opx in equilibrium with Gt (here referred to as Al-Opx thermobarometry) may be considerably more resistant to post-peak temperature reequilibration than Fe-Mg exchange thermometers (Aranovich and Podlesskii 1989; Anovitz 1991; Fitzsimons and Harley 1994; Pattison and Bégin 1994; Bégin and Pattison 1994). The interpretation that the Al-Opx thermometer may better record near-peak *P-T* conditions is based on observed compositional maps of Opx (Pattison and Bégin 1994), with particular attention to comparative Al-Opx vs. Fe-Mg thermometry, the results of which are extremely sensitive to thermometer calibrations.

The amount of Al_2O_3 entering orthopyroxene in the MAS system was experimentally calibrated as a function of pressure and temperature by Perkins et al. (1981), Gasparik and Newton (1984), and Aranovich et al. (1983) for garnet-, spinel-, and cordierite-bearing assemblages, respectively. Most recent studies have attempted to calibrate the *P, T,* and compositional dependence of Al_2O_3 in Opx in the system FeO-MgO-Al_2O_3-SiO_2 (FMAS), which more closely represents orthopyroxene occurrences in crustal rocks (e.g., Kawasaki and Matsui 1983; Harley 1984; Aranovich and Kosyakova 1984, 1987; Lee and Ganguly 1988; Eckert and Bohlen 1992). All these studies have demonstrated the large effect of Fe on Al_2O_3 solubility in Opx: in garnet-bearing assemblages Al_2O_3 decreases with increasing bulk Fe/Mg ratio, while in cordierite-bearing assemblages Al_2O_3 increases with increasing Fe/Mg. Unfortunately, there is no consensus among these studies in quantifying this effect. The data of Harley (1984) seem to indicate a very sharp decrease in Al-solubility, while those of Aranovich and Kosyakova (1984; 1987) suggest a rather smooth one; the other studies fall between these extremes.

A major drawback of the FMAS studies mentioned above is that, with the exception of three experimental brackets of Lee and Ganguly (1988), equilibrium was not demonstrated by reversals of the Al_2O_3 content of Opx approached from under- and oversaturation. Lack of reversed phase-equilibrium data makes modeling of the thermodynamic properties of Al-bearing Opx highly uncertain and prevents robust calibration of thermobarometers involving aluminous Opx. We became aware of

* Permanent address: Institute of Experimental Mineralogy, Chernogolovka, Russia.

0003–004X/97/0304–0345$05.00

TABLE 1. Chemical analyses (wt% and cations) and unit-cell edges of synthetic minerals

Phase	Alm	Fs	Al-Fs (avg.)	Al-Fs 1	Al-Fs 2	Al-Fs 3
No. of analyses	8	6	20	1	1	1
FeO*	43.05	54.61	51.86	50.59	54.08	51.31
Al_2O_3	20.38		5.08	5.24	2.99	5.91
SiO_2	36.00	45.76	42.84	42.75	44.30	42.24
Total	99.43	100.37	99.78	98.58	101.37	99.46
Si	2.99	1	0.93	0.94	0.95	0.92
Al	1.99		0.13	0.13	0.08	0.15
Fe	3.01	1	0.94	0.93	0.97	0.93
O	12	3	3	3	3	3
		Unit-cell parameters (Å)				
a	11.526(2)	18.442(3)	18.379(15)			
b		9.069(1)	9.017(13)			
c		5.235(1)	5.200(5)			
V	1531.2(6)	875.6(6)	861.8(16)			

Note: Analyses in last three columns show range of individual Al-Fs analyses. Uncertainties in the last digits are shown in parentheses.
* All Fe as FeO.

this uncertainty in the course of a thermodynamic analysis of high-temperature minerals in the system FMAST (Berman and Aranovich 1996) and found that this uncertainty severely affects the conclusions regarding the possibility of recovering near-peak temperatures of granulite-facies metamorphism with Al-Opx and Fe-Mg exchange thermometry. To help resolve these uncertainties in the primary experimental data as well as the ambiguities in applications, we present reversed experimental data that constrain thermodynamic properties of Fe-Al Opx by the equilibrium:

$$Fe_3Al_2Si_3O_{12}\ (Alm) = 3\ FeSiO_3\ (Fs) + Al_2O_3\ (Ok) \quad (1)$$

in which the orthopyroxene solid solution is expressed using the components ferrosilite (Fs) and orthocorundum (Ok = Al_2O_3). From an experimental standpoint, the advantage of employing this equilibrium is that it involves only one binary solid solution phase (Opx) whose equilibrium composition can be approached from opposite directions at fixed *P-T* conditions. Preliminary results of this study were reported by Aranovich and Berman (1995).

EXPERIMENTAL METHODS

Starting materials

Starting almandine garnet was prepared following the procedure suggested by Bohlen et al. (1983). First, almandine glass was obtained by melting 0.5 g of a stoichiometric mix of Fe_2O_3, Al_2O_3, and SiO_2 (all oxides as reagent-grade chemicals) in a graphite crucible at one atmosphere and 1300 °C for about 20 min. The glass had a homogeneous dark green color and was practically void of metallic Fe inclusions. Its chemical composition, determined by microprobe analysis exactly corresponded to almandine stoichiometry. Almandine was crystallized from the finely ground glass with the use of a graphite container in a piston-cylinder apparatus at 20 kbar and 1200 °C for approximately 24 h. No phases other than almandine were identified in the synthesis products. Unit-cell-edge measurements of the almandine determined by a slow scan of four X-ray reflections, (444), (640), (642), and (800), with synthetic corundum as an internal standard, yield a value $a_0 = 11.526$ (±0.002) Å (Table 1), in very good agreement with that determined for the Fe^{3+}-free garnet by Woodland and Wood (1989). Electron microprobe analysis of the synthetic garnet (Table 1) also showed excellent agreement with theoretical almandine stoichiometry, thus implying no significant Fe^{3+}.

End-member ferrosilite was crystallized from a mechanical mix of iron oxalate with silica in sealed gold capsules in a piston-cylinder device at 900 °C and 15 kbar for 24 h. Approximately 5 wt% excess SiO_2 was added to the ferrosilite mix to saturate the fluid phase that was formed on decomposition of iron oxalate with respect to silica. The synthesis products were relatively coarse-grained ferrosilite with subordinate amounts of quartz and graphite. No other phases were determined by optical, XRD, and BSE analysis. Presence of graphite precipitated from the C-O-H fluid phase during the syntheses indicates rather low f_{O_2} (about 1 log unit below the QFM buffer). Both unit-cell parameters and chemical composition of the synthetic ferrosilite (Table 1) suggest that little or no Fe^{3+} is present.

Orthopyroxene containing 5 wt% Al_2O_3 (Al-Fs) was synthesized in a two-step procedure similar to that suggested by Gasparik (1987) for making Al-rich Opx on the enstatite–Mg-Tschermak join. First, a mechanical mix of iron oxalate, silica, and γ-Al_2O_3 was melted in a sealed gold capsule at 1050 °C and 15 kbar in piston-cylinder apparatus for 30 min. Then the temperature was decreased to 950 °C, and the sample was held at this lower temperature for another 3 h. The synthesis products consisted of orthopyroxene, with minor quartz and graphite, and traces of fayalite as inclusions in the central parts of large Opx grains (Fig. 1a). No individual fayalite grains were identified by optical, XRD, SEM, or microprobe analysis. The aluminous Opx crystallized metastably (see discussion below regarding the stable assemblage at these

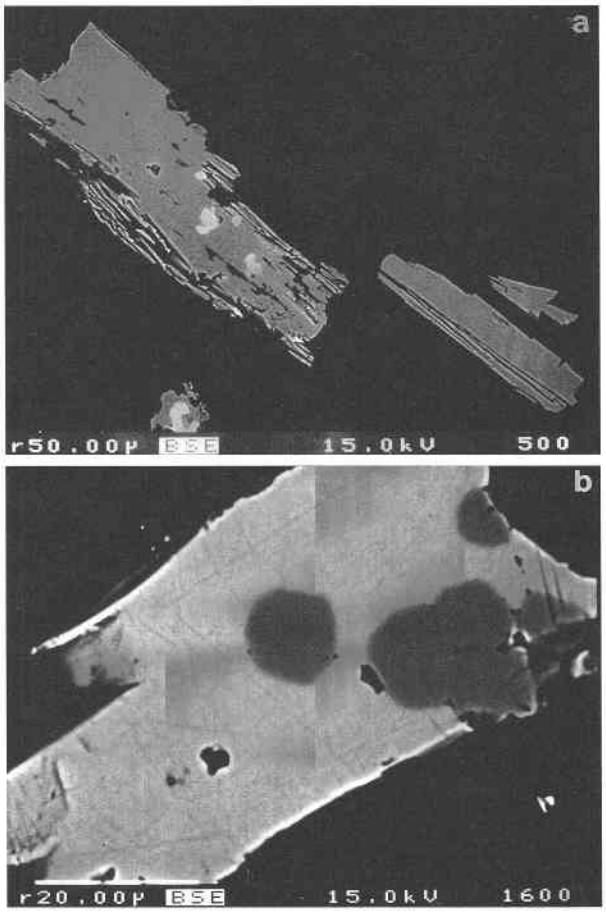

FIGURE 1. Backscattered electron images of synthesis and reversal experiment products: (**a**) synthetic Opx with 5 wt% Al_2O_3; bright spots are fayalite nuclei; (**b**) almandine (dark spots) and Opx (bright matrix) intergrowth in experiment 2b.

conditions) as large elongate grains with subordinate short prismatic grains. The crystals had a dark-green color and strong pleochroism, similar to pure ferrosilite. Their chemical composition ranged from 3.0–6.0 wt% Al_2O_3 (Table 1: Al-Fs #1–3), clustering at the nominal 5 wt% (Table 1). Unit-cell parameters, calculated from the *d* values of nine X-ray peaks that were given the same (*hkl*) indexes as corresponding peaks of pure ferrosilite, show systematic decrease from those of Fs (Table 1). Thus, introducing Al_2O_3 in the Fe-orthopyroxene has a similar, but somewhat greater effect on the Opx unit-cell volume in comparison with the MAS system. Large uncertainties in the measured unit-cell parameters of the Al-Opx (Table 1) are due to the inhomogeneous composition of the synthetic material used, which caused appreciable widening of the X-ray peaks.

Two starting mixes were used for the reversal experiments: one consisted of equal amounts of Alm and Fs (mix a in Table 2), and another of equal amounts of Alm and Al-Fs (mix b in Table 2). In a few experiments, we used the starting mix for the Al-Fs synthesis (mix c in Table 2), to compare the results of these synthesis experiments with other studies that used non-crystalline starting materials (Kawasaki and Matsui 1983; Harley 1984).

TABLE 2. Experimental data for Equilibrium 1

No.	*P* (kbar)	*T* °C	*t* (h)	Final X_{Ok}* range	Equilibrium X_{Ok}**
1a	15	950	70	0.007–0.015	0.015
1b	15	950	70	0.067–0.016	0.016
1c	15	950	94	0.009–0.018	
2a	15	1000	69	0.012–0.019	0.019
2b	15	1000	69	0.062–0.020	0.020
3a	15	900	141	0.005–0.012	0.012
3b	15	900	141	0.068–0.014	0.014
4a	15	850	169	0.000–0.010	0.010
4b	15	850	169	0.081–0.010	0.010
4c	15	850	188	0.008–0.016	
5a	12	950	120	0.010–0.017	0.017
5b	12	950	120	0.070–0.019	0.019
5c	12	950	144	0.014–0.020	
6a	10	900	167	Alm + Fa + Qz	
6b	10	900	167	Alm + Fa + Qz	
7a	12	850	144	0.000–0.012	0.012
7b	12	850	144	0.070–0.010	0.010
8a	20	1000	96	0.007–0.014	0.014
8b	20	1000	96	0.053–0.014	0.014
9a	20	900	96	0.004–0.010	0.010
9b	20	900	96	0.061–0.011	0.011
10a	20	1100	46	0.012–0.024	0.024
10b	20	1100	46	0.037–0.024	0.024

Note: All experiments contain Alm + Al-Opx, except for 6a and 6b; experiments 5a–5c also contain Fa.

* X_{Ok} = Al cations/2 on the 3-oxygen basis.

** Estimated equilibrium value based on most advanced Opx compositions.

In the reversal experiments, 3 to 4 mg of starting mix was loaded into ½-inch gold capsules along with 0.5–1.0 mg of hydrated oxalic acid and about 0.2 mg graphite powder. Capsules were then sealed by arc welding and placed in the high-pressure assembly described below. Experiments at 1100 °C, 20 kbar (Table 2) were made with no added flux to avoid melting.

Gold may dissolve a certain amount of Fe under the *P-T* conditions of the experiments. It was not significant, however, as might be deduced from the absence of any visible lightening of the charges at the capsule walls, as well as of any extra aluminous phases in the experiment products. Almandine was always present in experiment products, which ensured buffering of the reaction.

Apparatus and experiment procedure

All experiments were conducted in a conventional piston-cylinder apparatus with 19.01 mm diameter furnace assemblies and pistons. The assembly and technique for bringing *P-T* parameters of the experiments up to the required values exactly corresponded to those described in detail by R. C. Newton in Johannes et al. (1971) and Johannes (1973). Temperature was measured with W-Re thermocouples with no correction for the effect of pressure on emf. No pressure correction was applied to the NaCl assemblies in accord with the findings of many workers (e.g., Johannes et al. 1971). *P-T* fluctuations dur-

ing the experiments did not exceed 0.1 kbar and 1 °C. Overall uncertainties associated with the temperature gradient along the graphite heater and pressure calibration of the NaCl assembly are no greater than ± 5 °C and 0.4 kbar.

Two capsules, one containing mix a and the other mix b, were placed horizontally inside graphite cylinders and run simultaneously to eliminate possible differences in *P-T* conditions for each reversal experiment. Experiment duration varied from 2 d at 1100 °C to 6 d at 850 °C.

Experimental products

All experiment products were analyzed optically, by SEM, and by electron microprobe. X-ray diffraction was not used to analyze products of the reversal experiments to avoid grinding the samples, which could obscure any possible within-grain inhomogeneity of experiment products. Optical examination was found sufficient for identifying final phases in the experiments, primarily because of the distinct optical properties of the phases. The results of optical studies were always supported by back-scattered electron images and microprobe analysis.

Analyses were made using the University of Chicago Cameca SX-50 automated electron microprobe. Operating conditions were 15 kV accelerating potential and 25 nA current, measured by the Faraday cap. The electron beam was focused to less than 0.5 microns as determined by the spatial resolution in secondary electron images. The excitation volume (Reed 1993) can be calculated and for Fe is about 3.5 microns, with smaller values for the lighter elements (Al and Si) resulting from their lower critical excitation energy. X-ray intensities were obtained with the use of wavelength-dispersive spectrometers with backgrounds obtained by offsetting spectrometers on either side of the peak. Standards were synthetic enstatite with 5 wt% Al_2O_3 for Al and natural Fe-rich olivine for Fe and Si. Matrix corrections were those supplied by the manufacturer (PAP correction procedure). Estimated uncertainties of the analyses do not exceed 2% of the amount present for the major elements and 10% for the minor Al_2O_3 in Opx.

Special care was taken in selecting spots for microprobe analysis. Because of the same Fe:Si ratio in garnet and orthopyroxene, any possible overlap of the analyzed Gt and Opx grains would have produced artificial Opx compositions with high Al_2O_3 content. For each analyzed point, the sample was first imaged using secondary electrons to determine that the surface was polished flat. A backscattered electron (BSE) image was then used to verify the size of the analysis area and to allow accurate positioning of the beam: either the center of the smaller grains or near the edge of larger grains to determine zoning. It was always possible to avoid probing the composite spots overlapping in the plane of the sample because of contrasting BSE images of Gt and Opx (Fig. 1b). The above procedure, however, cannot eliminate composite spots from very thin grains composed of two phases where a second phase lies just below the surface. Edge effects either because of adjacent phases of different composition or rounding of polished edges were minimized by not obtaining analyses closer than 3 microns to the edge determined on BSE images.

Individual analyses were accepted if oxide totals were 100 ± 2% and stoichiometries did not deviate by more than 1.5% in any cation site from ideal almandine or orthopyroxene mineral formulae. With these criteria applied, no appreciable Fe^{3+} in either garnet or orthopyroxene was indicated in the microprobe analyses. Very good agreement between calculated octahedral and tetrahedral Al atoms in Opx provided an additional indication of the high quality of the accepted analyses.

Experimental results

A major difficulty in interpreting the results of experiments on solid-solution–bearing equilibria in systems containing Al_2O_3 arises from compositional inhomogeneity of experiment products (e.g., Perkins et al. 1981; Aranovich and Kosyakova 1984; Aranovich and Pattison 1995). We also encountered this problem in our study. Opx from any single experimental charge varied in composition both within individual grains and from grain to grain. The intergranular compositional heterogeneity was found to be more pronounced than zoning within crystals, indicating that the major mechanism of equilibration was dissolution-precipitation by a fluid phase rather than solid-state diffusion (e.g., Koziol and Newton 1989; Pattison 1994).

In each experiment, 20–30 grains of Opx were analyzed. Most grains were too small to be searched for zoning. Only for a few larger grains, like that shown in Figure 1b, was it possible to collect spot analyses on both inner and outer parts of the grains. For these grains compositional variations were always consistent with the expected reaction progress. In the experiments with starting mix a, rims were more Al-rich than the cores, while in the runs with starting mix b, rims were less Al-rich. If the variations were artifacts caused by analysis of overlapping Gt and Opx grains, only rimward increases in Al would have been observed in experiments with both types of starting material.

A group (not less than 4 individual points) of spot analyses, either of separate homogeneous grains or of the rims of zoned grains, representing compositions most different from the starting ones, were assumed to be closest to equilibrium. The average of these compositions, along with experiment conditions, are given in Table 2 and shown in Figure 2. With the exception of experiments 4a and 7a at the lowest temperature, we did not observe pure Fs in experiments with starting mix a, whereas most runs using mix b contained some Opx grains with Al contents indistinguishable from that of Al-Fs. This contrast indicates that the forward reaction rate is faster than the backward reaction. Such asymmetry in the rates of forward and backward reactions seems to be a typical feature of solid-solution reactions (e.g., Aranovich 1976; Aranovich and Pattison 1995). One implication is that midpoints of

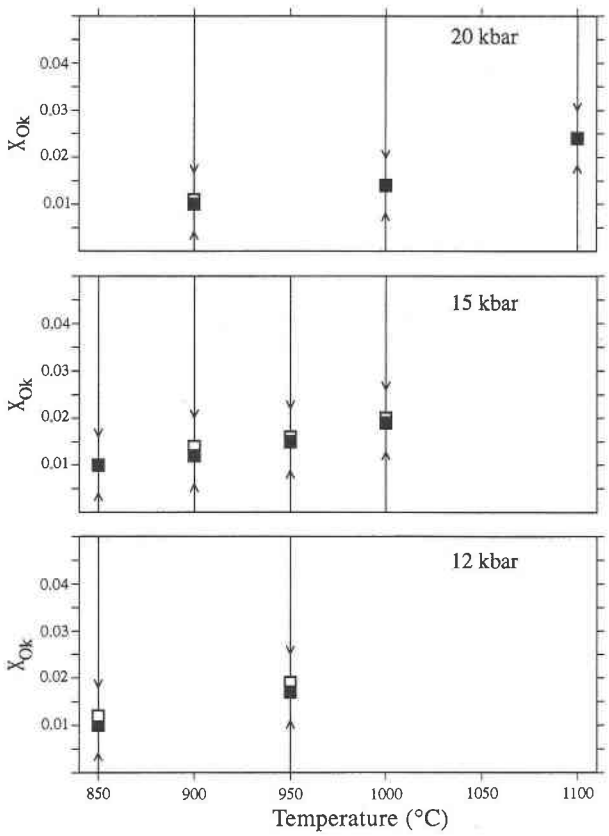

FIGURE 2. Reversals of Al_2O_3 content of Fe-Opx, expressed as mole fraction of orthocorundum (Ok) component. All experiment product compositions (squares) were approached from high-Al (open symbols) and low-Al (solid symbols) Opx starting materials.

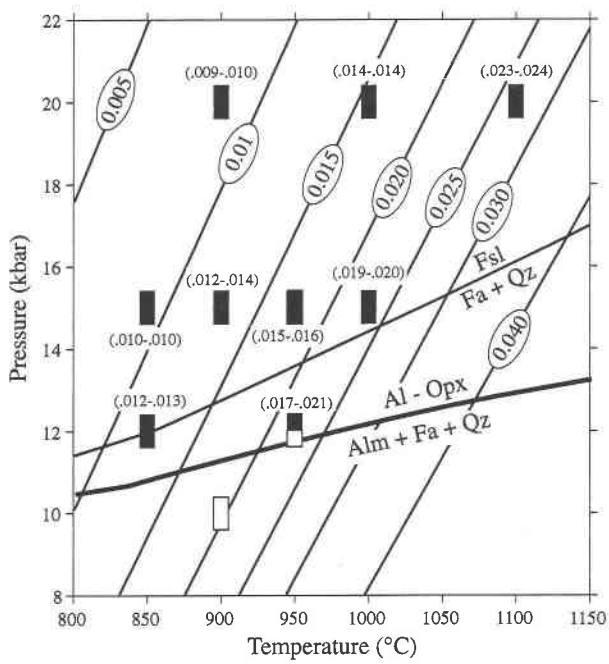

FIGURE 3. Experimental results constraining the equilibrium: Alm = 3 Fs + Ok (1). Size of boxes shows experimental *P-T* uncertainties, with nominal width of X_{Ok} brackets in parentheses. Experiments produced the assemblages: Opx + Gt (solid), Opx + Gt + Fa (half-filled box), and Gt + Fa + Qz (open box). Isopleths of X_{Ok}; Fsl = Fa + Qz equilibrium, and FeO-Al_2O_3-SiO_2 univariant phase boundary (heavy curve) calculated as described in text.

compositional brackets for these reactions may not represent the most probable equilibrium position (as is assumed in least-squares methods of fitting phase-equilibrium data).

Unlike the results obtained on similar reactions in MAS (e.g., Perkins et al. 1981; Aranovich and Kosyakova 1984), our data show almost no overlapping of the most advanced compositions of Opx in the coupled experiments (Fig. 2). This observation is most likely explained by faster reaction rates for both half-reactions in the FAS compared with the MAS system. In addition, microprobe analysis of FAS experiment products was helped by the greater difference in atomic numbers between Al and Fe compared to Mg and Al.

Also presented in Table 2 are the results of a few synthesis-type experiments that used as a starting material the same mechanical mix used for the Al-Opx synthesis. With sufficient duration, these experiments produced low-Al Opx and almandine, suggesting that syntheses of Al-Fs involved metastable growth of higher Al Opx (~5% Al_2O_3) during much shorter experiment times. The compositional range of the resulting Opx (Table 2) was generally not as large as that in the experiments using the crystalline starting mixes, but in all cases the range spanned that of the equilibrium value determined with the crystalline materials. Thus, although the results produced by the synthesis experiments are consistent with those produced with crystalline starting materials, knowing the direction of compositional approach to equilibrium with the latter materials yields a more precise estimate of equilibrium compositions.

Our data indicate very limited solubility of Al_2O_3 (< 0.025 X_{Ok}) in Fe-Opx, which is significantly lower than that in Mg-Opx (~0.06 X_{Ok}) under the same *P-T* conditions. This result is consistent with the much larger stability field of almandine relative to pyrope and the much smaller stability field of ferrosilite relative to enstatite. Unfortunately, we have been able to collect data on Equilibrium 1 over a rather restricted range of *P-T* conditions. At higher temperatures we observed melting of Alm in presence of H_2O-CO_2 fluid. At lower pressure, Al-free Opx decomposes to Fa+Qz (Bohlen et al. 1980; Bohlen and Boettcher 1981). In the FAS system, the lower pressure limit of Opx stability is defined by the univariant reaction (Fig. 3):

$$2[(x)\mathrm{FeSiO3} + (1 - x)\mathrm{Al_2O_3}] = (4x - 3)\mathrm{Fe_2SiO_4} + 2(1 - x)\mathrm{Fe_3Al_2Si_3O_{12}} + (4x - 3)\mathrm{SiO_2}.$$

In experiments at 950 °C and 12 kbar (5a, 5b in Table 2; Fig. 3) we observed fayalite in run products. Although the above equilibrium has not been reversed, we believe that these conditions are very close to the univariant equilibrium for the following reasons. First, both half-reversal experiments produced very similar final Opx compositions (X_{Ok} = 0.017–0.019), which implies that Opx was stable. Second, the calculated position of this equilibrium, using thermodynamic properties that do not incorporate constraints on its location, is within 200 bars of these nominal *P-T* coordinates (Fig. 3).

Discussion

The phase-equilibrium data presented above provide important constraints on the position and slope of isopleths of Opx Al_2O_3 content in the FAS system. Figure 3 shows isopleths computed with thermodynamic data based on the data presented in this study in addition to a large body of other experimental data for FMAS minerals. Derivation of the thermodynamic data (available from Berman) incorporates uncertainties in *P, T,* and composition and is discussed in detail elsewhere (Berman and Aranovich 1996). Of primary importance is that the Al_2O_3 solubility in FAS based on the new experiments agrees well with the value based on the lone other reversal (at 50 ± 4 kbar and 1300 °C) by Kawasaki and Matsui (1983). Also important is the conclusion (Berman and Aranovich 1996) that the present experimental data are completely compatible with the only other reversed Al_2O_3 solubilities of Opx in equilibrium with garnet, in the MAS (Lane and Ganguly 1980; Perkins et al. 1981) and FMAS (three brackets by Lee and Ganguly 1988) systems. Lastly, although the thermodynamic properties were optimized to experimental results including those of Harley (1984), we note here (and discuss further below) that his data are not bracketed from high- and low-Al starting materials and thus are in need of additional experimental verification. The Berman and Aranovich (1996) thermodynamic data also indicate that the Al_2O_3 content of Opx in the most Fe-rich experiments by Aranovich and Kosyakova (1984) were overestimated by about 20–50% (relative) probably because of metastable formation of high-Al Opx. Taken together, our results suggest that quantitative calculations applied to natural FMAS Opx can now be much more reliably performed.

For Al-Opx thermometry based on Equilibrium 1, the following simplified equation (using average ΔH^0, ΔS^0, ΔV^0 values) has been derived from the thermodynamic data obtained by Berman and Aranovich (1996):

$$T(\mathrm{K}) = \frac{-\Delta H^0_a - 3H^x_{Fs} - H^x_{Ok} + H^x_{Alm} - P(\Delta V^0_a - 3V^x_{Fs} - V^x_{Ok} + V^x_{Alm})}{\mathrm{R}\ln K_a - \Delta S^0_a - 3S^x_{Fs} - S^x_{Ok} + S^x_{Alm}} \quad (2)$$

with

$$K_a = \frac{X^3_{Fs} X_{Ok}}{X^3_{Alm}}. \quad (3)$$

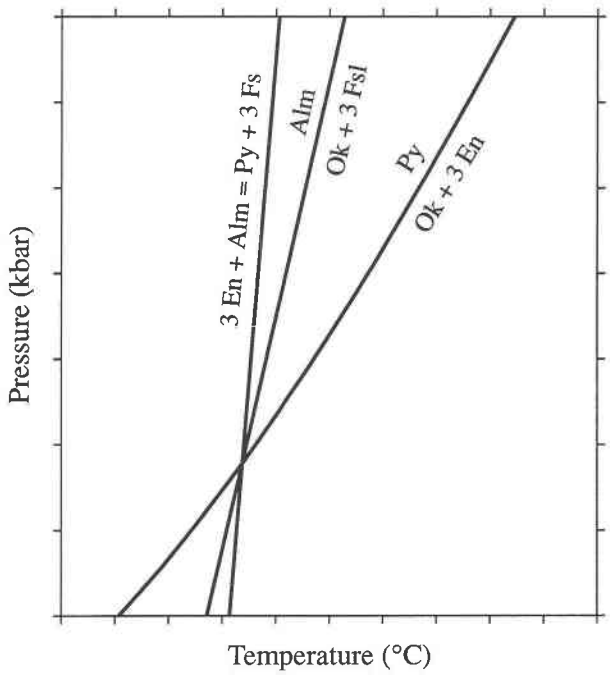

Figure 4. Model invariant point geometry that dictates that, at all pressures other than the invariant point, the MAS Equilibrium 4 yields more discordant temperatures than the FAS Equilibrium 1, compared to the Fe-Mg exchange thermometer (Equilibrium 5). *P-T* of invariant point changes with different mineral compositions.

Numerical values for all terms in Equation 2 are given in the Appendix. We recommend that this equation not be used outside of the *P-T* window 600–1100 °C at 2–20 kbar. More accurate calculations should be performed with thermodynamic data given by Berman and Aranovich (1996).

The FAS Equilibrium 1 investigated in this study is linearly related to an equivalent MAS equilibrium

$$\mathrm{Py} = 3\ \mathrm{En} + \mathrm{Ok} \quad (4)$$

that intersects the Fe-Mg exchange equilibrium between Opx and Gt

$$\mathrm{Py} + 3\ \mathrm{Fs} = \mathrm{Alm} + 3\ \mathrm{En} \quad (5)$$

at an invariant point (Fig. 4). Compared with the MAS Equilibrium 4, the FAS Equilibrium 1 has a considerably larger enthalpy and entropy of reaction, which makes it a much more robust thermobarometer. The MAS equilibrium has a shallower slope than the FAS equilibrium (Fig. 4), a difference that dictates that it will always produce poorer agreement with the exchange Equilibrium 5 than Equilibrium 1, except if pressure estimates yield the invariant point. Under optimal circumstances, intersection of Equilibria 1 and 5 define *P* and *T* uniquely, but the acute angle of intersection of these equilibria is not conducive to reliable *P-T* determinations. A better approach is to use a net-transfer equilibrium involving garnet and plagioclase as a barometer and to retrieve *T* estimates

from comparison of the positions of Equilibria 1 and 5. Of particular importance is the relative insensitivity of Equilibrium 1 to Fe-Mg ratio, in comparison with Equilibria 4 and 5. For example, a 0.01 change in garnet Fe-Mg ratio translates to temperatures that are about 10, 30, and 60 °C different for Equilibria 1, 4, and 5, respectively. As a consequence, temperatures based on Equilibrium 1 should be the least sensitive to any resetting of Gt or Opx compositions that might occur in a slowly cooling metamorphic terrain.

Recent applications, using an equivalent of the MAS Equilibrium 4 involving Tschermak's component (here referred to as Equilibrium 4a) and Harley's experimental data as a basis of calculations (Bégin and Pattison 1994), have concluded that Al-Opx yields significantly higher *P-T* results than the Fe-Mg exchange equilibrium. These results are consistent with compositional maps of Opx that show greater zonation in Fe-Mg ratio than Al_2O_3 contents (Pattison and Bégin 1994), and that have been attributed to diffusional reequilibration at lower than peak temperatures. Following a correction procedure suggested by Fitzsimons and Harley (1994) based on pressure differences recorded by Equilibrium 4a and the Gt-Opx-Plag-Qz barometer, Bégin and Pattison (1994) estimate the amount of Fe-Mg reequilibration from the difference in temperatures computed with Equilibria 4a and 5. Peak temperatures are then recomputed from Opx and Gt compositions adjusted for this late Fe-Mg exchange. With this technique, temperature values up to 300 °C higher than unadjusted Fe-Mg exchange temperatures were computed for some paragneisses from the Minto Block, northern Quebec (Bégin and Pattison 1994), and up to 140 °C higher for the East Antarctica rocks (Fitzsimons and Harley 1994). As quantitative results of these studies rely to a large extent on Harley's (1984) calibration of the Equilibria 4a and 5, we first compare Harley's experimental data with the thermodynamic data derived by Berman and Aranovich (1996).

Figure 5 shows the results of this comparison expressed as a difference between the temperature values of Harley's experiments ($T_{experimental}$ in Fig. 5) and those calculated from his reported Gt and Opx compositions with the thermodynamic data based in part on the experiments presented here ($T_{calculated}$). Readily apparent from Figure 5 is the large discrepancy between Harley's experimental data and our calibration of Equilibria 4 (open triangles) and 5 (open squares), while much better agreement is observed between his data and calculations based on Equilibrium 1 (filled circles). As noted above, temperature calculations based on Reactions 4 and 5 are extremely sensitive to the input compositions. If we assume that synthesis experiments by Harley produced non-equilibrium Fe-rich garnet, which is known to nucleate more readily, it would explain the large positive differences based on Reaction 5 and large negative differences based on Reaction 4. The much less sensitive Reaction 1 gives $T_{calculated}$ in good agreement (most differences <100 °C) with the experimental observations. Hence we consider

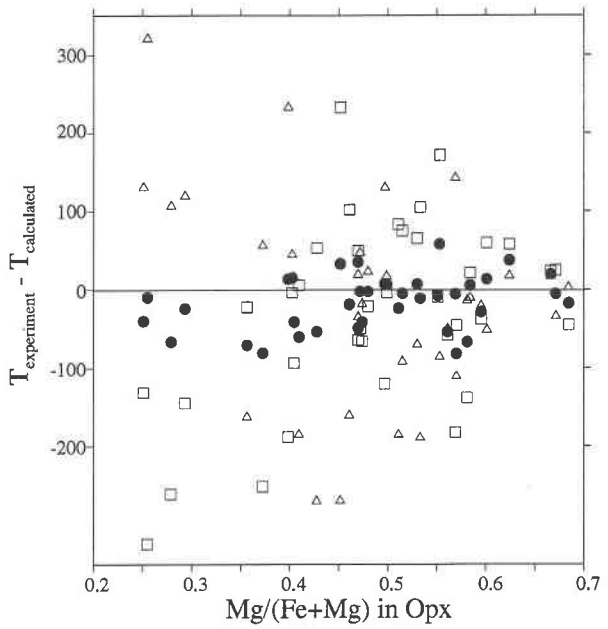

FIGURE 5. Comparison of predicted and measured temperatures for Gt-Opx pairs produced experimentally by Harley (1984). Note close correspondence of temperatures calculated with Equilibrium 1 (solid circles) compared with Equilibria 4 (triangles) and 5 (squares). See text for discussion.

that, although Fe-Mg ratios may not be correct, the Al_2O_3 contents of Opx reported by Harley (1984) are probably close to equilibrium values. We emphasize, however, that further work is needed to substantiate this conclusion because none of his data are bracketed from high- and low-Al starting Opx, and Berman and Aranovich's (1996) analysis of Aranovich and Kosyakova's (1984) experiments involving FMAS Opx indicates large overstepping of equilibrium Al_2O_3 contents.

Figure 6 shows some results of thermobarometric calculations using the thermodynamic data derived by Berman and Aranovich (1996). For Minto Block, North Quebec samples studied by Bégin and Pattison (1994), we compute temperatures with Equilibrium 1 (solid circles in Fig. 6) that are 55–130 °C higher than Fe-Mg exchange temperatures (open diamonds in Fig. 6). Thermobarometric results for Furua Complex samples (Coolen 1980) show tighter clustering with all but one rock yielding 850 ± 50 °C with Equilibrium 1 while Fe-Mg exchange temperatures are lower by 50–75 °C for all but one sample. Taken as a whole, the results for both regions support previous suggestions (Aranovich and Podlesski 1989; Fitzsimons and Harley 1994; Bégin and Pattison 1994) that Al_2O_3 solubility in Opx is less susceptible to post-thermal peak reequilibration. The less-pronounced compositional zoning profiles for Al_2O_3 compared with Fe-Mg in Opx grains adjacent to garnet documented by Pattison and Bégin (1994) are due to a smaller dX/dT for Al_2O_3 relative to Fe/(Fe+Mg) ratio in Opx, combined with a difference in closure of the two thermometers. Larger dif-

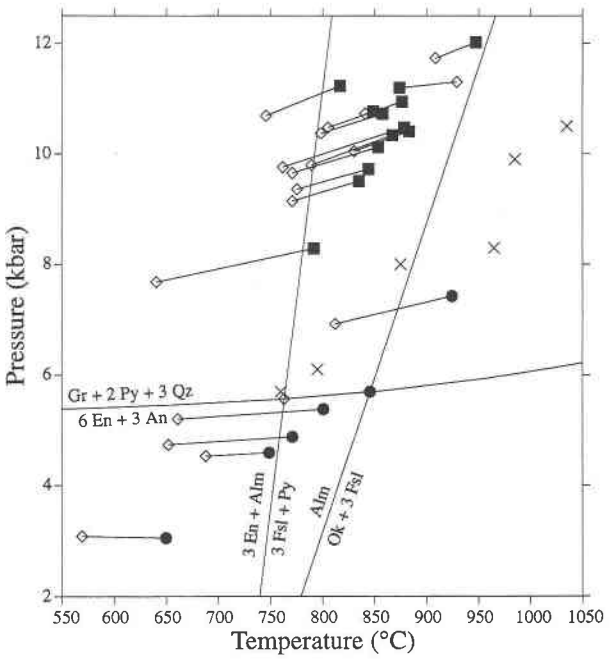

FIGURE 6. Computed *P-T* results for Opx-Gt samples from the Minto block (circles; Bégin and Pattison 1994) and the Furua Complex (squares; Coolen 1980). *P-T* results are based on intersection of the Opx-Gt-Plag-Qz barometer with the Alm = Ok + Fsl equilibrium (solid symbols) or with the Fe-Mg exchange equilibrium (open diamonds). Curves shown for Minto sample number C10B. Crosses show *P-T* results of Bégin and Pattison (1994) for Minto block samples after correction for inferred late Fe-Mg exchange (see text for discussion).

ferences in closure temperature would be expected from samples that experienced higher peak temperatures and slower cooling histories, but calculated temperatures will, of course, be sensitive to textural characteristics of individual samples, such as grain size and proximity of Opx-Gt grains.

A problem that deserves more attention is whether thermobarometry applications with Equilibrium 1 should incorporate compositional readjustments to remove the effects of late Fe-Mg exchange, as suggested by Bégin and Pattison (1994). In principal, readjustment to obtain the same temperatures with Equilibria 1 and 5 is reasonable, but a practical difficulty is that computed differences between these equilibria for many samples are within or near the combined uncertainties of such calculations. For Equilibrium 1, enough uncertainty remains in the slope of Al isopleths determined in this experimental study (Fig. 3) that different optimizations of the experimental data analyzed by Berman and Aranovich (1996) yield temperatures computed with Equilibrium 1 at 5–6 kbar that are as much as 25 °C lower than presented here. For Equilibrium 5, different optimizations can yield temperatures up to 40 °C higher than computed with the thermodynamic data presented by Berman and Aranovich (1996).

With this magnitude of uncertainty remaining, compositional adjustments aimed at removing the effects of retrograde Fe-Mg exchange may well overestimate the amount of Fe-Mg reequilibration and yield temperatures that are spuriously high. Associated pressures, assumed to close at the same temperature as Equilibrium 1, would also be erroneously high. For example, the Minto Block core compositions tabulated by Bégin and Pattison (1994) yield temperatures (filled circles in Fig. 6) that are lower with Equilibrium 1 by 30–120 °C than computed by Bégin and Pattison (1994) with the Harley and Green (1982) Al thermometer, while pressures are within 1.4 kbar. In contrast, Bégin and Pattison's (1994) results incorporating their compositional adjustment for estimated Fe-Mg reequilibration (crosses in Figure 6) are as much as 200 °C and 3.5 kbar higher than our results shown in Figure 6. Until further work reduces the uncertainties in the application of Equilibria 1 and 5 to natural samples, we recommend a more conservative approach to Al-Opx thermometry in which mineral compositions are adjusted by the minimum amount required to yield temperature differences between Equilibria 1 and 5 that are less than combined uncertainties (~75 °C) in the positions of Equilibria 1 and 5.

ACKNOWLEDGMENTS

L.Y.A.'s work on this project was supported by the NSF grant EAR-9310264 (to R.C. Newton) and ISF (Soros Foundation) grant JIJ-000 (to LYA). Bob Newton's very helpful advice regarding experiments is greatly appreciated. We also thank Ian Steele for his generous help with the microprobe analyses and Joe Pluth for assistance with XRD measurements. This is Geological Survey of Canada contribution no. 1996433.

REFERENCES CITED

Anovitz, L.M. (1991) Al zoning in pyroxene and plagioclase: Window on late prograde to early retrograde *P-T* paths in granulite terranes. American Mineralogist, 76, 1328–1343.

Aranovich, L.Y. (1976) Phase correspondence in the system epidote-garnet according to experimental data. In V.A. Zharikov and V.V. Fed'kin, Eds., Contributions to physico-chemical petrology, p. 14–33. Nauka Press, Moscow (in Russian).

Aranovich, L.Y., Kosyakova, N.A., and Van, K.V. (1983) Experimental study of the equilibrium cordierite + orthopyroxene + quartz in the system $MgO-Al_2O_3-SiO_2$. Doklady Akademii Nauk SSR, 269, 1174–1177 (in Russian).

Aranovich, L.Y., and Kosyakova, N.A. (1984) Experimental study of the equilibrium: cordierite + orthopyroxene + quartz in the system $FeO-MgO-Al_2O_3-SiO_2$. Doklady Akademii Nauk SSR, 274, 399–401 (in Russian).

——— (1987) The cordierite = orthopyroxene + quartz equilibrium: laboratory data on and thermodynamics of ternary Fe-Mg-Al orthopyroxene solid solutions. Geochemistry International, 24, 111–131.

Aranovich, L.Y., and Podlesskii, K.K. (1989) Geothermobarometry of high-grade metapelites: simultaneously operating reactions. In R.A. Cliff, B.W.D. Yardley, and J.S. Daly, Eds., Evolution of metamorphic belts, p. 45–62. Blackwell Scientific Publications, Oxford.

Aranovich, L.Y., and Berman, R.G. (1995) Al_2O_3 solubility in orthopyroxene in equilibrium with almandine in the $FeO-Al_2O_3-SiO_2$ system. Current Research of the Geological Survey of Canada Paper, 1995-E, 271–278.

Aranovich, L.Y., and Pattison, D.R.M. (1995) Reassessment of the garnet-clinopyroxene Fe-Mg exchange thermometer: I. Reanalysis of the Pattison and Newton (1989) run products. Contributions to Mineralogy and Petrology, 119, 20–31.

Bégin, N.J., and Pattison, D.R.M. (1994) Metamorphic evolution of granulites in the Minto block, northern Quebec: extraction of peak *P-T* conditions taking account of late Fe-Mg exchange. Journal of Metamorphic Geology, 12, 411–428.

Berman, R.G., and Aranovich, L.Y. (1996) Optimized standard state and mixing properties of minerals: I. Model calibration for olivine, orthopyroxene, cordierite, garnet, and ilmenite in the system FeO-MgO-CaO-Al_2O_3-SiO_2-TiO_2. Contributions to Mineralogy and Petrology, 126, 1–24.

Bohlen, S.R., Essene, E.J., and Boettcher, A.L. (1980) Reinvestigation and application of olivine-orthopyroxene-quartz barometry. Earth and Planetary Science Letters, 47, 1–10.

Bohlen, S.R., and Boettcher, A.L. (1981) Experimental investigations and geological applications of orthopyroxene geobarometry. American Mineralogist, 66, 951–964.

Bohlen, S.R., Wall, V.J., and Boettcher, A.L. (1983) Experimental investigations and geological applications of equilibria in the system FeO-TiO_2-Al_2O_3-SiO_2-H_2O. American Mineralogist, 68, 1049–1058.

Boyd, F.R. (1973) A pyroxene geotherm. Geochimica et Cosmochimica Acta, 37, 2533–2546.

Coolen, J.J.M. (1980) Chemical petrology of the Furua granulite complex, southern Tanzania. Gemeente Universiteit Amsterdam, 13, 1–258.

Eckert, J.O., and Bohlen, S.R. (1992) Reversed experimental determinations of the Mg-Fe^{2+} exchange equilibrium in Fe-rich garnet-orthopyroxene pairs. Transactions of American Geophysical Union, 73, 608.

Fitzsimons, I.C.W., and Harley, S.L. (1994) Disequilibrium during retrograde cation exchange and recovery of peak metamorphic temperatures: A study of granulites from Antarctica. Journal of Petrology, 35, 543–576.

Gasparik, T. (1987) Orthopyroxene thermobarometry in simple and complex systems. Contributions to Mineralogy and Petrology, 96, 357–370.

Gasparik, T., and Newton, R.C. (1984) The reversed alumina contents of orthopyroxene in equilibrium with spinel and forsterite in the system MgO-Al_2O_3-SiO_2. Contributions to Mineralogy and Petrology, 85, 186–196.

Harley, S.L. (1984) The solubility of alumina in orthopyroxene coexisting with garnet in FeO-MgO-Al_2O_3-SiO_2 and CaO-FeO-MgO-Al_2O_3-SiO_2. Journal of Petrology, 25, 665–696.

Harley, S.L., and Green, D.H. (1982) Garnet-orthopyroxene barometry for granulites and peridotites. Nature, 300, 697–701.

Johannes, W. (1973) Eine vereinfachte piston-zylinder-apparatur hoher genauigkeit. Neues Jahrbach für Mineralogie Monatshefte, 7/8, 337–351.

Johannes, W., Bell, M., Mao, H.K., Boettcher, A.L., Chipman, D.W., Hays, J.F., Newton, R.C., and Seifert, F. (1971) An interlaboratory comparison of piston-cylinder pressure calibration using the albite-breakdown reaction. Contributions to Mineralogy and Petrology, 32, 24–38.

Kawasaki, T., and Matsui, Y. (1983) Thermodynamic analyses of equilibria involving olivine, orthopyroxene and garnet. Geochimica et Cosmochimica Acta, 47, 1661–1679.

Koziol, A.M., and Newton, R.C. (1989) Grossular activity-composition relationships in ternary garnets determined by reversed, displaced phase equilibrium experiments. Contributions to Mineralogy and Petrology, 103, 423–433.

Lane, D.L., and Ganguly, J. (1980) Al_2O_3 solubility in orthopyroxene in the system MgO-Al_2O_3-SiO_2: A reevaluation, and mantle geotherm. Journal of Geophysical Research, 85, 6963–6972.

Lee, H.Y., and Ganguly, J. (1988) Equilibrium compositions of coexisting garnet and orthopyroxene: Experimental determinations in the system FeO-MgO-Al_2O_3-SiO_2, and applications. Journal of Petrology, 29, 93–113.

Pattison, D.R.M. (1994) Are reversed Fe-Mg exchange and solid solution experiments really reversed? American Mineralogist, 79, 938–950.

Pattison, D.R.M., and Bégin, N.J. (1994) Compositional maps of metamorphic orthopyroxene and garnet: Evidence for a hierarchy of closure temperatures and implications for geothermometry of granulites. Journal of Geology, 12, 387–410.

Perkins, D., Holland, T.J.B., and Newton, R.C. (1981) The Al_2O_3 contents of enstatite in equilibrium with garnet in the system MgO-Al_2O_3-SiO_2 at 15-40 kbar and 900–1600 °C. Contributions to Mineralogy and Petrology, 78, 99–109.

Reed S.J.B. (1993) Electron microprobe analysis, second edition. 326 p. Cambridge University Press, Cambridge, U.K.

Woodland, A.B., and Wood, B.J. (1989) Electrochemical measurements of the free energy of almandine $Fe_3Al_2Si_3O_{12}$ garnet. Geochimica et Cosmochimica Acta, 53, 2277–2282.

Manuscript received March 6, 1996
Manuscript accepted November 20, 1996

Appendix: Thermodynamic parameters for use with Equation 2

$\Delta H^0_a = 72767$ J

$\Delta S^0_a = 16.79$ J/K

$\Delta V^0_a = 1.58$ J/bar

Ferrosilite (Fs)

$$H^x = -2600x_{En}^2 - 32398.4x_{Ok}^2 - 13120.4x_{En}x_{Ok}$$

$$S^x = -1.342x_{En}^2 - 1.342x_{En}x_{Ok}$$

$$V^x = -0.883x_{Ok}^2 - 0.497x_{En}x_{Ok}$$

Orthocorundum (Ok)

$$H^x = -21878.4x_{En}^2 - 32398.4x_{Fs}^2 - 51676.4x_{En}x_{Fs} + 26534.9x_{Fs}/(x_{Fs} + x_{En})$$

$$S^x = 1.342x_{En}x_{Fs} + 16.111x_{Fs}/(x_{Fs} + x_{En})$$

$$V^x = -0.386x_{En}^2 - 0.883x_{Fs}^2 - 1.269x_{En}x_{Fs} + 0.175x_{Fs}/(x_{Fs} + x_{En})$$

Almandine (Alm)

$$H^x = 5064.5(x_{Py}^2 - 2x_{Py}^2x_{Alm}) + 6249.1(x_{Alm}x_{Py} - 2x_{Py}x_{Alm}^2) - 66940x_{Gr}^2x_{Py} - 136560x_{Gr}x_{Py}^2 + 21951(x_{Gr}^2 - 2x_{Gr}^2x_{Alm}) + 11581.5(x_{Gr}x_{Alm} - 2x_{Gr}x_{Alm}^2) + 73298(x_{Gr}x_{Py} - 2x_{Gr}x_{Py}x_{Alm})$$

$$S^x = 4.11(x_{Py}^2 - 2x_{Py}^2x_{Alm}) + 4.11(x_{Alm}x_{Py} - 2x_{Py}x_{Alm}^2) - 18.79x_{Gr}^2x_{Py} - 18.79x_{Gr}x_{Py}^2 + 9.43(x_{Gr}^2 - 2x_{Gr}^2x_{Alm}) + 9.43(x_{Gr}x_{Alm} - 2x_{Gr}x_{Alm}^2) + 32.33(x_{Gr}x_{Py} - 2x_{Gr}x_{Py}x_{Alm})$$

$$V^x = 0.01(x_{Py}^2 - 2x_{Py}^2x_{Alm}) + 0.06(x_{Alm}x_{Py} - 2x_{Py}x_{Alm}^2) - 0.346x_{Gr}^2x_{Py} - 0.072x_{Gr}x_{Py}^2 + 0.17(x_{Gr}^2 - 2x_{Gr}^2x_{Alm}) + 0.09(x_{Gr}x_{Alm} - 2x_{Gr}x_{Alm}^2) + 0.281(x_{Gr}x_{Py} - 2x_{Gr}x_{Py}x_{Alm})$$